ELSEVIER

0958-9465(95)00029-1

Cement & Concrete Composites **18** (1996) 239–249

0958-9465/96/$15.00

Toughening in Cement Based Composites. Part II: Fiber Reinforced Cementitious Composites

Victor C. Li & Mohamed Maalej

Advanced Civil Engineering Materials Research Laboratory, Department of Civil and Environmental Engineering, The University of Michigan, MI 48109-2125, USA

Abstract

This paper reviews the mechanisms of toughening in fiber reinforced cement based composites. Reference is made to frontal, crack tip and wake processes, and estimates of contributions to composite toughness of the individual mechanisms are included. It is emphasized that the wake processes, which dominate the inelastic energy absorption during fracture development in these materials, can be well characterized by tensile stress vs crack opening relationships. The fiber/matrix interface debonding energy, not usually important in fiber reinforced concrete, is shown to play an important role in new straining–hardening engineered cementitious composites as an additional frontal process with significant energy absorption capacity, thus giving rise to a cement based material with extremely high damage tolerance. © 1996 Elsevier Science Limited.

Key words: Toughening mechanisms, fiber debonding, frictional sliding, plastic yielding, snubbing, matrix spalling, fiber bridging, aggregate bridging, multiple cracking, strain hardening.

INTRODUCTION

In recent years, it has become clear that the use of fibers in cement based composites leads to a significant toughening effect, much more so than improvements in the strength properties for which the fibers were originally intended for in the early days of fiber reinforced concrete (FRC). Thus serious efforts are now underway to design these brittle matrix composites with toughness values that are orders of magnitude higher than that of regular cement or concrete (e.g. Refs 1 and 2). To achieve this objective, tailoring of the fiber, matrix and interface requires knowledge of how these three phases interact in the composite such that a large amount of energy is absorbed in the inelastic process. Attempts are being made at this moment to bring this knowledge to bear on the performance of structures built partially or fully with such composites (e.g. Refs 3 and 4).

The present paper attempts to identify the micromechanisms responsible for toughening in fiber reinforced cementitious composites, based on direct or indirect experimental observations of the failure process of these materials. Estimation of the level of toughness contributions are also indicated based on micromechanics studies. (The toughening mechanisms in unreinforced cementitious materials have been reviewed in Part I of this paper.)

TOUGHENING MECHANISMS IN FIBER REINFORCED CONCRETE

In this section, we review a variety of fiber/matrix interactions which contribute to composite toughening, and the σ–δ curve of fiber bridging with and without aggregates. The discussion will focus on randomly oriented discontinuous fibers typically used in FRCs.

Fiber/matrix interactions

There are several types of fiber/matrix interactions which lead to energy absorption in the fiber bridging zone of an FRC. These include interface debonding, frictional sliding, and inclined angle effects associated with random fiber orientations (e.g. Refs 5 and 6). Although the amount of energy associated with each

mechanism for a single fiber may not be significant, the large amount of fibers, bridging over an extended length can contribute an enormous toughening effect to the composite. Figure 1 shows the large bridging zone of such an FRC. The end of the bridging zone is associated with fibers being pulled out of the matrix. This is typical of steel and polymer fiber reinforced concrete. For composites with brittle fibers such as carbon, the end of the bridging zone is associated with the rupturing of fibers.

Fiber debonding involves the breakdown of the material in the interfacial zone due to interfacial shear resulting from the pulling of a fiber bridging a matrix crack. Figure 2 shows an image of an interface being debonded, with the debonded zone indicated by the distorted pattern of the Moiré fringes.[7] The debonding process can be strength or fracture controlled depending on the physical nature of the fiber/matrix interface.[8] In a composite, the discontinuous random fibers can be expected to have different embedment lengths. However, when the crack opening is small, most of the fibers can be assumed to be undergoing debonding. The resulting $\sigma-\delta$ will then be ascending. Measurement of this part of the curve in a uniaxial tension test is not usually conducted, since the load would have exceeded the maximum bridging stress when the matrix cracks in a typical FRC, resulting in a sudden load drop and a crack opening largely in the descending branch of the $\sigma-\delta$ curve. Parts of this curve, however, can be obtained by tracking the load–crack opening on one of the multiple cracks in a uniaxial tension test of a pseudo strain-hardening FRC. This is possible since in such a composite, the material can continue to carry higher load after matrix first crack.[9–10] Figure 3 shows some experimental data points of the $\sigma-\delta$ curve of a strain-hardening nylon fiber reinforced cement. The corresponding theoretical curve is from Li:[11]

$$\sigma_f(\tilde{\delta})=\sigma_o\left[2\left(\frac{\tilde{\delta}}{\tilde{\delta}^*}\right)^{1/2}-\frac{\tilde{\delta}}{\tilde{\delta}^*}\right] \text{ for } 0\le\tilde{\delta}\le\tilde{\delta}^* \quad (1)$$

where $\sigma_o=g\tau V_f(L_f/d_f)/2, \tilde{\delta}=\delta/L_f/2)$, and where $\tilde{\delta}^*=(2\tau/E_f)(L_f/d_f)/(1+\eta)$ corresponds to the maximum attainable value of δ_o (normalized by the half fiber length $L_f/2$) for the fiber with the longest possible embedment length of $L_f/2$. In the above, $\eta=(V_fE_f)/(V_mE_m)$, E_m and V_m stands for the Young's modulus and volume fraction of

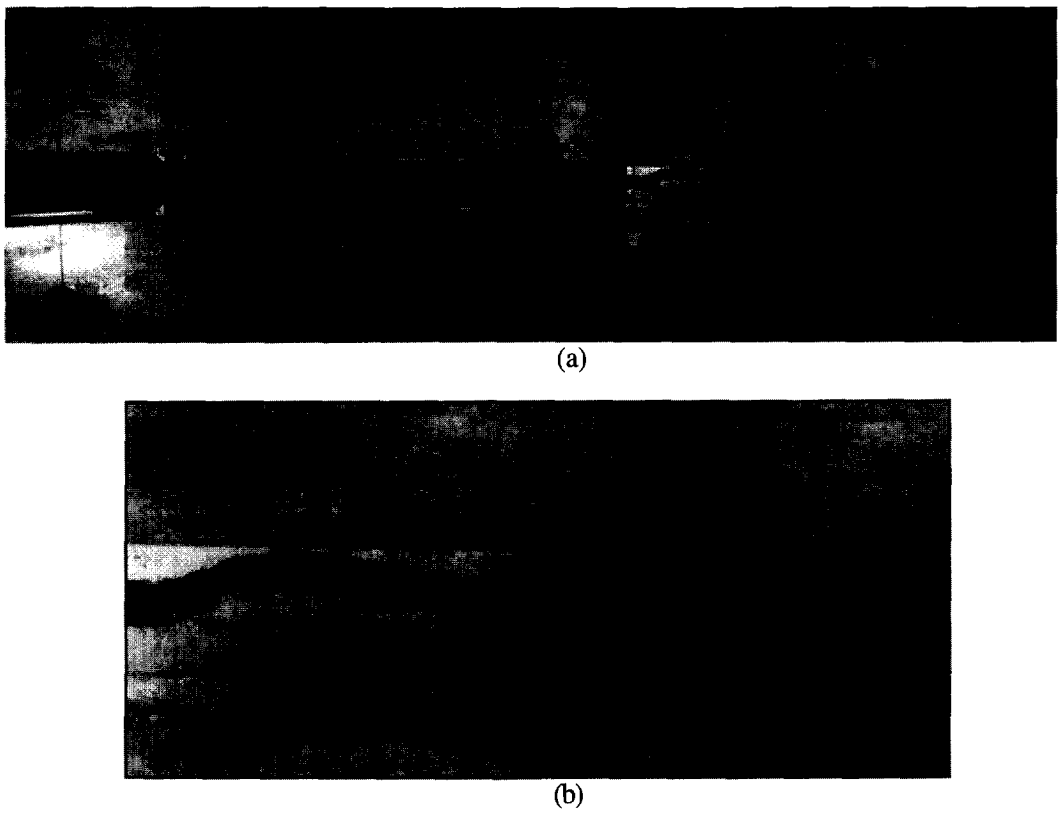

(a)

(b)

Fig. 1. Crack wake of an FRC showing extensive fiber bridging. Area enclosed in box in (a) shown magnified in (b).

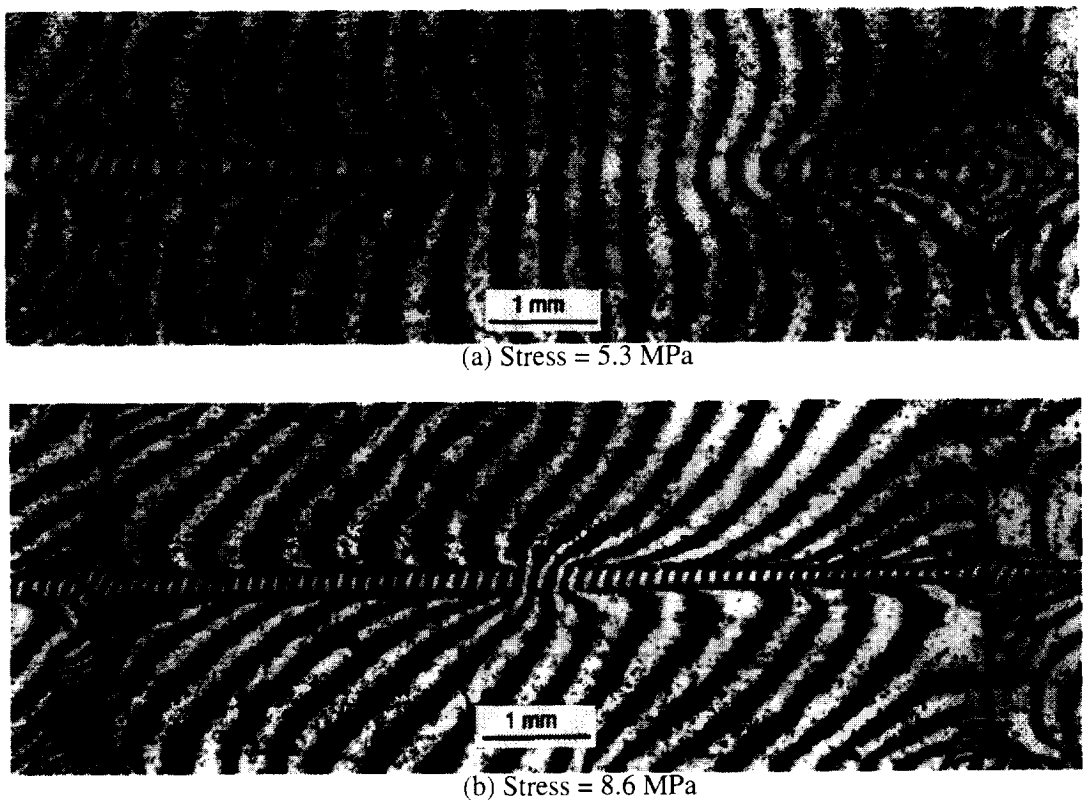

Fig. 2. Fiber debonding as imaged by Moiré interferometry.[7]

the matrix material which contains the fibers. E_f, d_f and τ are the Young's modulus, diameter and interface bond strength of the fiber. The snubbing factor g is defined in terms of the snubbing coefficient f:

$$g=\frac{2}{4+f^2}\left(1+e^{\pi f/2}\right) \qquad (2)$$

More on the snubbing factor and coefficient will be given later. In (1), it has been assumed that the interface debond process is governed by a single level interfacial strength τ. A corresponding equation can be obtained when the debond is governed by interface fracture process with the corresponding fracture energy Γ.

The fiber debonding energy can be estimated by integrating the area under the pre-peak σ–δ curve [eqn (1)] if the interface property is known. Li[11] showed that for the case of strength control interface, this energy is given by

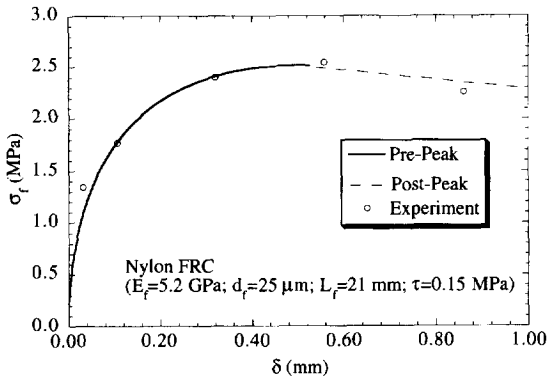

Fig. 3. Ascending branch of σ–δ data for Nylon FRC. Theoretical curve from eqn (1).

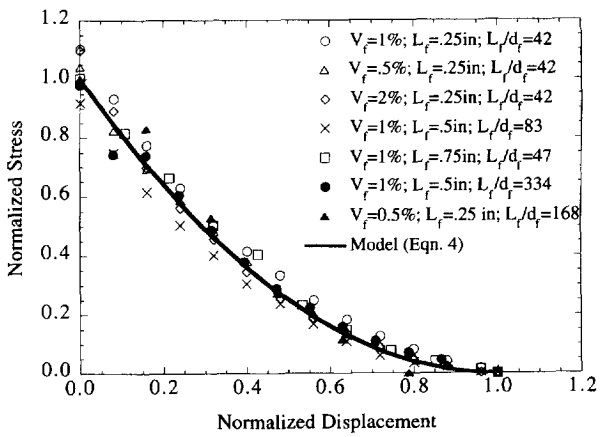

Fig. 4. Softening branch of σ–δ for a variety of FRCs. Data from Refs 12 and 23; theoretical curve from eqn (4).

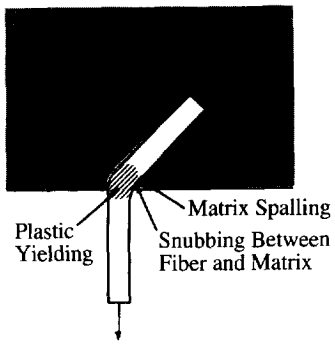

Fig. 5. Inclined fiber bridging a matrix crack showing possible mechanisms of fiber yielding at bend, snubbing and matrix spalling.

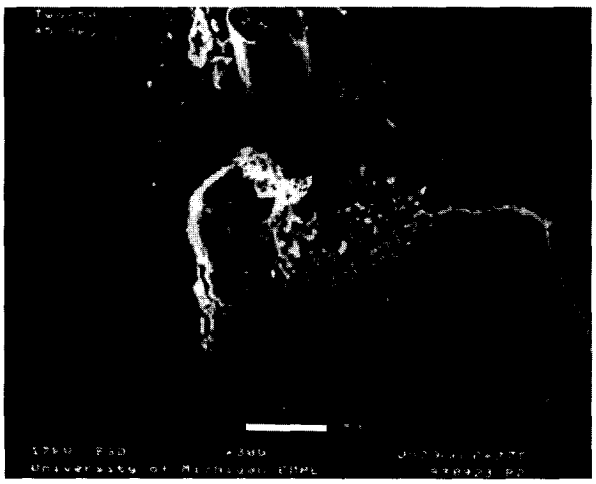

Fig. 6. Spalling of cementitious matrix under indentation loading of an inclined fiber.

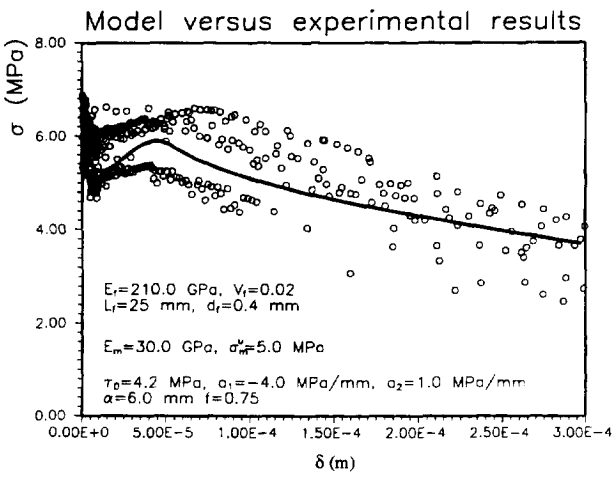

Fig. 7. Combined $\sigma-\delta$ data and model of aggregate and fiber bridging.

$$G_r=\frac{5}{12}g\tau V_f d_f\left(\frac{L_f}{d_f}\right)^2\tilde{\delta}^* \tag{3}$$

When the crack opening is large, most fibers would be fully debonded, and frictional sliding or pull-out of these fibers would occur towards the end of the crack wake. This corresponds to the descending branch of the $\sigma-\delta$ curve for FRCs in a uniaxial tension test. Experimental determination of this branch of the $\sigma-\delta$ curve for a variety of FRCs has been extensively reported. This softening branch has been very well modeled, both empirically[12,13] and theoretically.[11] The analytic expression for the $\sigma-\delta$ curve based on constant frictional pull-out is given by

$$\sigma_f(\tilde{\delta})=\sigma_o[1-(\tilde{\delta}-\tilde{\delta}^*)]^2 \text{ for } \tilde{\delta}^*<\tilde{\delta}\leq 1 \tag{4}$$

Equation (4) has been found to compare favorably with a wide variety of experimental data for both steel and polymeric FRC materials, as shown in Fig. 4. This suggests that the frictional pull-out concept of fibers bridging a matrix crack is reasonably accurate. Refinement of the friction concept has been offered by Wang *et al.*[14] with regard to slip-hardening or weakening behavior of fiber/matrix interfaces which suffer damage due to the sliding process. The process of slip-hardening has the potential of further toughening the FRC. Unfortunately, in most cases, the fiber abrasion damage process requires extensive sliding (several mm) to reach a significant level.

The fracture energy contribution based on constant friction sliding can be determined by integrating the area under the post-peak $\sigma-\delta$ curve [eqn (4)]. This energy component is given by

$$G_c=\frac{1}{12}g\tau V_f d_f\left(\frac{L_f}{d_f}\right)^2 \tag{5}$$

In both (3) and (5), a 3-D orientation has been assumed. Further, all fibers are assumed to pull-out rather than fracture. For a typical FRC, the pull-out energy would be of the order of several kJ/m^2. This is at least one order of magnitude larger than the fracture energy of cement or concrete. However, it should be noted that to access this high level of fracture energy, it is necessary to pull the fibers out completely, implying a large bridging zone and

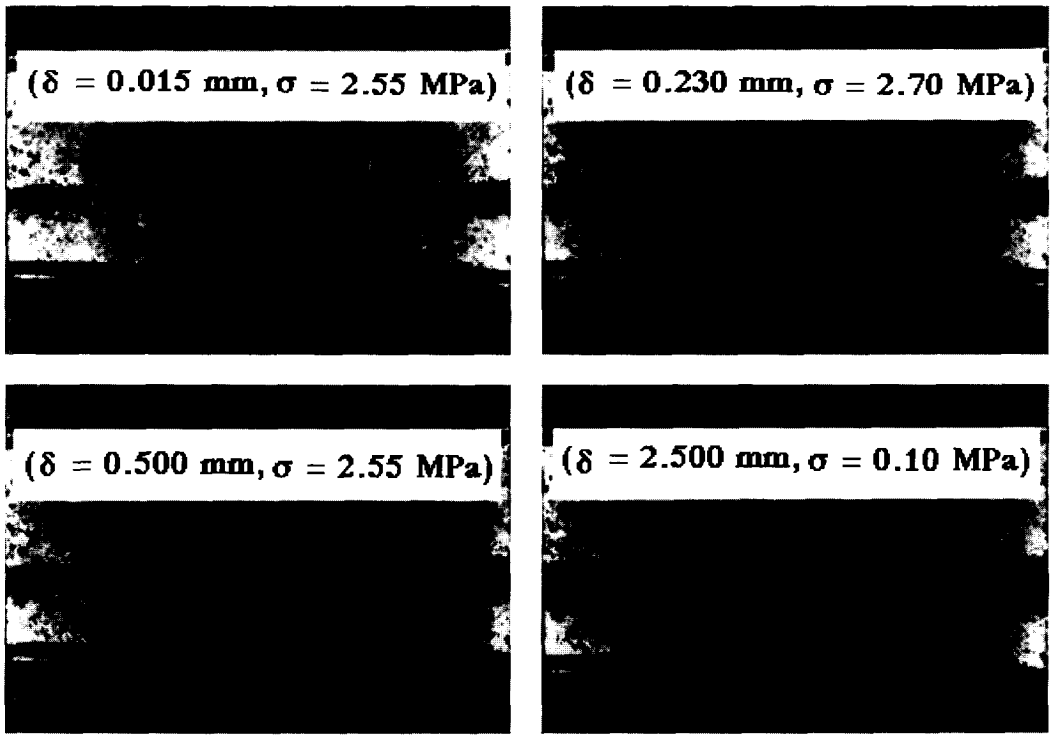

Fig. 8. Photographs of cracking process at different stages of uniaxial tensile loading in an FRC.

large crack opening on the order of mm to cm scale. Such large crack opening is not acceptable for normal serviceability in most practical structures.

Comparison between (3) and (5) indicates that the value of G_r/G_c is of the order of $\tilde{\delta}^*$. This is a very small value (of the order of 10^{-3}, for $\tau/E_f \sim 10^{-3}$ and $L_f/d_f \sim 10^2$), so that for most FRCs, this contribution to the composite toughness due to interface debonding can be ignored.

Apart from debonding and pull-out, additional interactions between fiber and matrix occur when the fibers are randomly oriented. When fibers cross a matrix crack at an inclined angle (Fig. 5), it is necessary for the fiber to bend so that the bridged segment of the fiber will be parallel to the tensile loading direction. The energy absorbed in the bending process necessarily depends on the type of fiber. For example, Morton[6] found that for steel fibers which plastically yield under bending, the amount of fracture energy consumption can be dominated by work due to the plastic bending process. The relative magnitude of this energy to the total fracture energy including that due to fiber pull-out [eqn (5)] will depend on the fiber and interface parameters. For low aspect ratio fibers and/or low bond strength fibers, G_c in (5) will be small, and the bending energy which depends only on the fiber yield strength will be important. The significance of flexural yielding will diminish for composites with fibers of large aspect ratio and high interfacial strength.

When fibers are brittle, such as in the case of carbon fibers, the effect of bending actually leads to fiber failure at lower bridging load in comparison to the aligned fiber case.[15] This cuts short the debonding and pull-out processes, and leads to lower energy consumed in the bridging zone. In the case of polymer fibers which yield at very low stress, the energy consumed due to fiber flexural yielding again can be expected to be small.

Another effect of inclined fibers is snubbing.[16] This effect is best visualized by considering a flexible fiber bearing on the matrix as it exits into the matrix crack as a rope passing over a friction pulley. This additional local friction effect is dependent on the fiber tension and therefore the fiber aspect ratio and interface bond strength, unlike that of flexural yielding described above. Indeed this coupling of tension and bending makes snubbing a multiplying effect, as opposed to the additive effect associated with plastic yielding considered by Morton.[6] That is, as the interface is strengthened or if the fiber aspect ratio is increased, the snubbing contribution also increases. This mechanism is quantified by the snubbing factor

g in (5). The value of g ranges from 1 to 2.3.[11,16] In the case of $g=2$, for example, the snubbing effect doubles the fracture energy of the case without snubbing effect.

It should be noted that while the energies associated with fiber flexural yielding and snubbing derive from fibers inclined to the matrix crack, random fiber orientation also reduces the number of fibers bridging across the matrix crack. This can result in a lower bridging energy level, as appears to be supported by experiments.[5]

Another mechanism associated with inclined bridging fibers is matrix spalling (Fig. 5). The

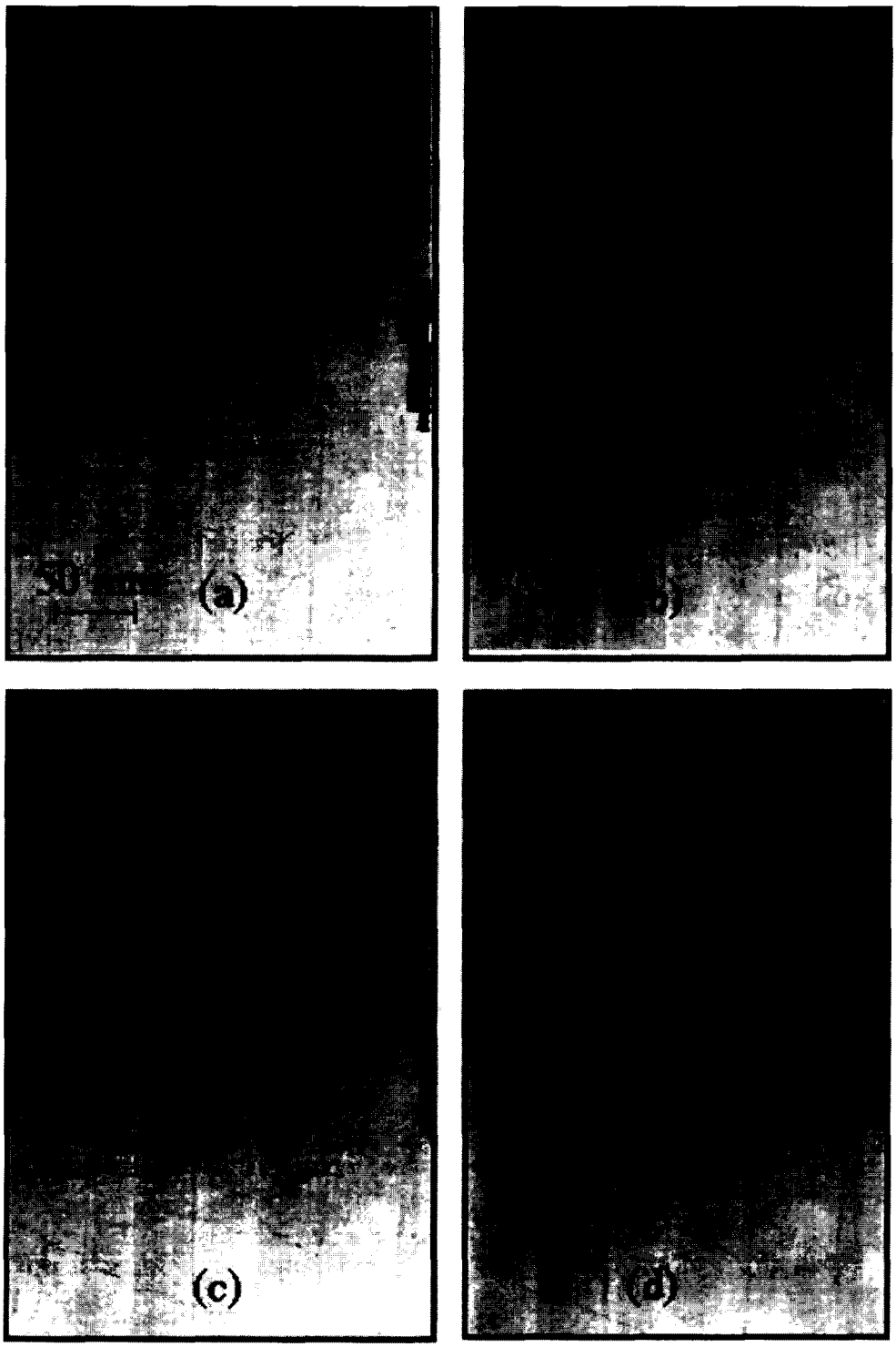

Fig. 9. Damage zone development at four stages of loading in a double cantilever beam specimen; (a) $\delta_L=3.10$ mm, (b) $\delta_L=7.32$ mm, (c) $\delta_L=19.45$ mm and (d) $\delta_L=23.16$ mm.

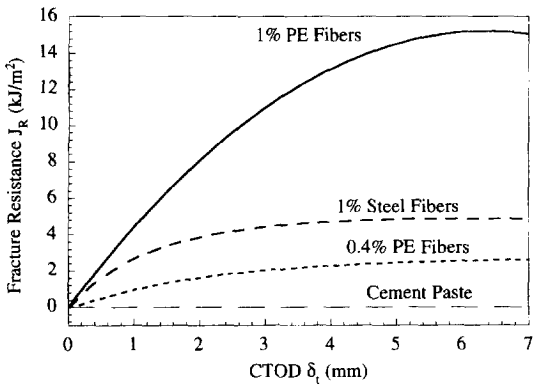

Fig. 10. R-curve behavior of ECC and FRC.

mechanics giving rise to the snubbing effect also cause a local indentation load acting on the matrix. As a result, the matrix may split under the indentation load and form a wedge spall. An SEM micrograph of such a spall obtained under an inclined fiber pull-out test is shown in Fig. 6. While this indentation process causes inelastic energy absorption, the energy contribution by this spalling mechanism is difficult to identify because of its interacting mechanisms with the bridging fiber. Matrix spalling is expected to release fiber tension and therefore lower the bridging stress. This may in fact lower the energy consumption in the bridging zone. On the other hand, for brittle fibers, matrix

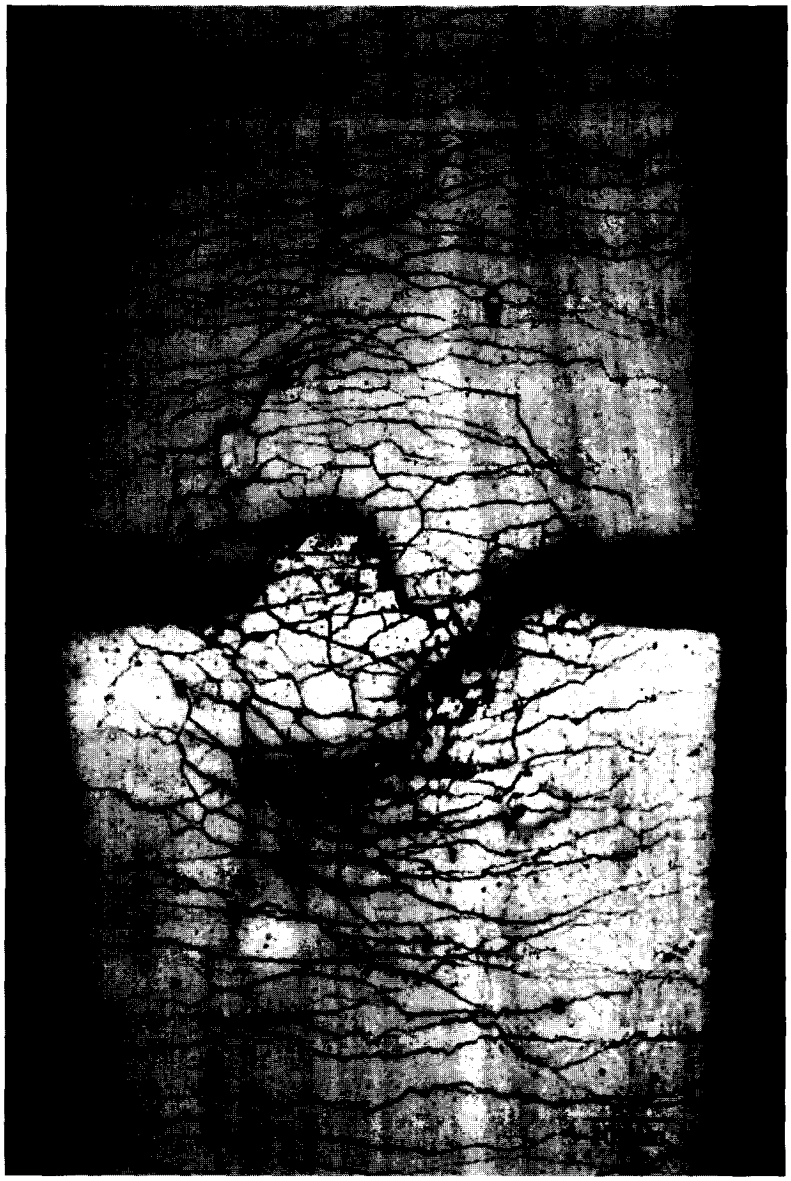

Fig. 11. Damage pattern of a shallowly double-edged, notched specimen of an ECC which shows a notch-insensitive failure mode.

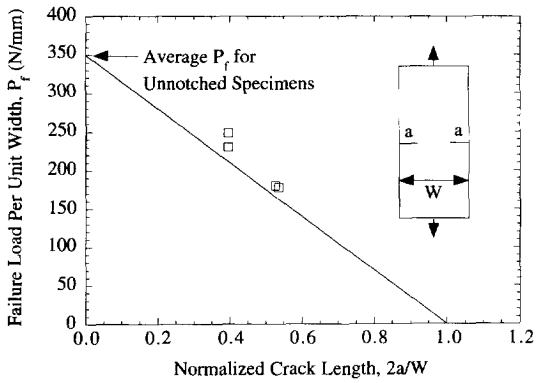

Fig. 12. Failure load vs notch depth relation confirming notch-insensitivity of ECC materials.

spalling may allow survival of the brittle fiber by lowering the stress in the brittle fiber, and therefore lead to an extension of the σ–δ curve which would have otherwise been cut short by fiber rupture.

Combined effect of aggregate and fibers

It is interesting to consider the combined effect of aggregate and fibers acting simultaneously in the crack wake. This was carried out recently[17] in the form of σ–δ curves measurements and modeling for steel and PP-FRCs (Fig. 7). The modeling combines in essence the concepts of aggregate tension-softening (see Part I) and fiber bridging [eqns (1) and (4)], with further additional refinements. Figure 8 shows a series of photographs at different stages of cracking in the uniaxial tension specimen. Although effects of interactions between the aggregates and fibers may be expected, especially for large size aggregates or high fiber volume fractions composites, Fig. 7 appears to support a simple additive contribution of the aggregate and fibers to bridging toughening in the crack wake.

TOUGHENING IN STRAIN HARDENING CEMENT BASED COMPOSITES

In this section, we review recent observations of a new toughening mechanism in strain hardening cement based composites. The material has been designed based on micromechanical principles so that strain-hardening occurs despite a relatively low fiber volume fraction (typically less than 2%). We have called such a material an Engineered Cementitious Composite (ECC). Detailed information on ECC can be found in Ref. 10 and in the references given below. The toughening mechanism leads to a high toughening level in cement based composites while at the same time reveals an R-curve behavior different from that of ordinary FRCs. Development of a large damage zone and behavior of notch insensitivity are discussed.

Damage tolerance

Figure 9 shows four stages of damage zone development on a large double cantilever beam fracture specimen.[2,18] Advance of a main crack from the initial notch was significantly delayed and can only be observed (Fig. 9(d)) after an extensive damage zone off the main crack plane has been developed. It appears that the notch tip was rapidly blunted by the damage process, analogous to the process of dislocation blunting in a ductile metal. Notch tip blunting relaxes the strain-concentration, allowing further loading to be applied before real crack growth can begin. This crack growth process is very different from that of ordinary FRCs. Fracture energy as high as 27 kJ/m^2 has been measured for an ECC with 2% fiber volume fraction. It was experimentally determined that a little more than 50% ($\approx$15 kJ/m^2) of this energy comes from inelastic damage process occurring over an extended volume of material, covering an area dimension of more than 1000 cm^2 on the specimen surface.[18] The rest of the fracture energy derives from fiber pull-out process in the crack wake as given in eqn (5). The inelastic damage process involves micro-cracking of the matrix and the associated fiber bridging on these cracks. Because this composite shows strain-hardening behavior under uniaxial tension, it is expected that the microcracks observed in the damage zone are associated with the multiple cracking in the uniaxial tensile specimens. Indeed, Horii and co-workers (personal communications, 1994) recently confirmed through a FEM-BEM simulation that material strain-hardening is occurring in the damage zone as it develops.

Based on the above discussion, energy consumed in the damage zone should derive mostly from the debonding process of bridging fibers. If this were the case, the ratio of off-crack plane fracture energy to on-crack plane fracture energy should be given by

$$R=\frac{G_r A_d}{G_c A_m}\approx 1 \qquad (6)$$

where A_d and A_m are the area of microcracks in the damage zone and area of main crack, respectively. G_r and G_c are the pre-peak and post-peak fiber bridging energies given by eqns (3) and (5). Photographic evidence indicates that A_d=5400 cm^2 and A_m=87 cm^2, whereas G_r and G_c are estimated to be 0.17 kJ/m^2 and 9.9 kJ/m^2 based on an interfacial bond strength τ of 0.7 MPa and a snubbing factor g of 2.0. These numbers imply that the ratio $R\approx 1.1$ confirming the concept that the fiber debonding mechanism in the frontal process zone is indeed contributing as much as the familiar bridging mechanism in the wake process to composite toughness in this ECC. Thus, the interface debonding energy not usually significant in an FRC plays an important toughening role in an ECC. The blunting effect of the microcracking frontal process in ECC renders the material highly damage tolerant.

R-curve behavior

The R-curve behavior of any composite with wake processes reflects the increasing amount

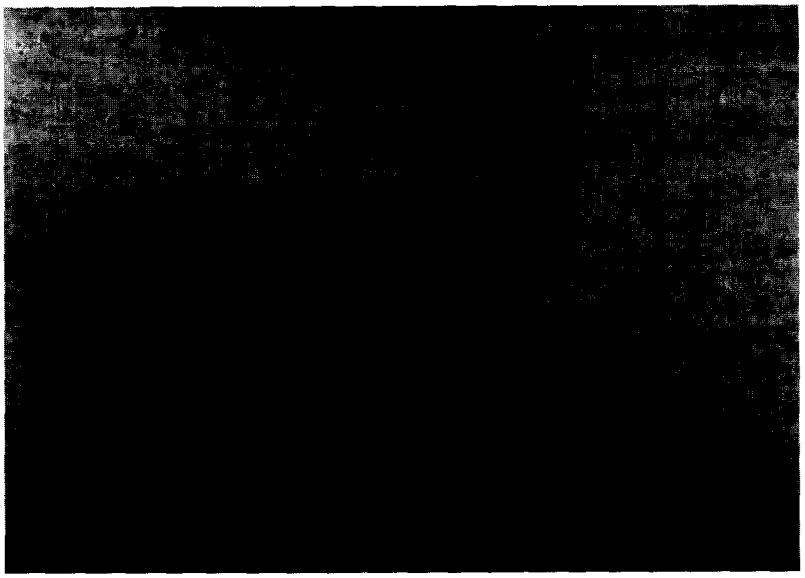

(a)

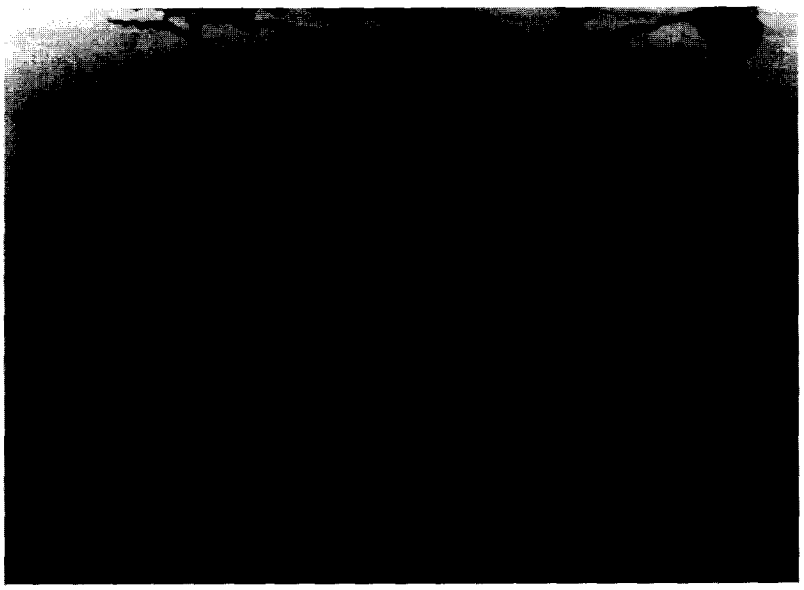

(b)

Fig. 13. Crack pattern of R/C beams loaded to failure.[22] Beam (a) has a regular concrete cover, and beam (b) has an ECC cover.

of fracture energy absorbed as the wake zone grows. Typically an effective crack length increment is associated with the increasing compliance due to the growing wake. In an FRC, the R-curve behavior is then directly associated with the σ–δ bridging process[19] described in the previous section. In an ECC, this bridging process is still effective, but is superimposed by the additional energy absorption associated with the damage process off the crack plane. Hence we expect that the R-curve in an ECC will rise sharper than the corresponding FRC. This concept was tested by Li *et al.*[20] Figure 10 shows the test results of a DCB specimen of an ECC with 1% polyethylene (PE) fibers. The R-curve plots the J-value obtained from the J-based determination technique described in Ref. 21 against the opening of the crack tip δ_t. The crack tip opening is used in place of the crack length increment because extension of the crack is difficult to determine due to its often non-planar growth.

For comparison, a 1% steel fiber and 0.4% PE fiber FRCs (both do not show strain-hardening under uniaxial tension test) are also included in Fig. 10. It is clear that the R-curve of the ECC rises much more rapidly, confirming the concept of energy absorption as discussed above. Further, the steady state value for the 1% PE ECC is more than 2.5 times that of the 0.4% PE FRC. This again reflects that additional energy is consumed outside of the main crack plane on which fiber pull-out occurs.

Notch insensitivity

An implication of the large damage zone prior to fracture localization is that the ligament in a notched specimen must be at least as large as the dimension of this zone to observe fracture behavior (fracture dominated failure mode). Otherwise the material will show notch insensitivity, i.e. the strength of the specimen will become insensitive to the presence of the notch. Limited test results of a double edged notch specimen appear to support this idea. Figure 11 shows the damage effect on the ligament in the specimen. The microcrack pattern appears as a plastically yielded zone and extensive microcracking occurs over the whole length of the specimen. Figure 12 shows the net section strength line, confirming that this specimen did not suffer from brittle fracture failure.

A practical implication of the notch insensitivity behavior of this material could be in the enhancement of structural durability of R/C structures. In this type of structure, durability often suffers from large crack openings in the concrete cover, steel corrosion, and subsequent concrete spalling. Since concrete covers are typically of the dimension of several cms, which is smaller than the damage zone size of the strain-hardening material, a fracture can never be fully developed. Instead, it is expected that an expanding zone of microcrack damage will occur. In regular R/C structures, fracture will still be restrained by the reinforcing steel, but the R/C structure with an ECC layer will have microcrack width which is self-restrained. This concept is illustrated by Fig. 13, which shows the crack pattern of a regular R/C beam and that of an ECC layered beam[22] loaded under flexure. Microcracks on the ECC cover show a crack width an order of magnitude smaller than that on the regular concrete cover. Thus the damage tolerance of ECC can be advantageous in enhancing structural performance.

CONCLUSIONS

In this paper, the toughening mechanisms of cement based composites are reviewed. In concrete the major wake process appears to be associated with aggregate/ligament bridging. In FRC, the major wake process appears to be associated with fiber pull-out against friction modified by inclined fiber bridging effects. A Cohesive Crack Model is seen to describe the inelastic wake action of aggregates in concrete, whereas a Bridged Crack Model is seen to be appropriate to describe those of fibers in FRC. In either case, energy absorption in the wake processes generally dominate over those of the frontal processes. On a macroscopic level, wake processes can be characterized by stress vs crack opening (σ–δ) curves obtained from uniaxial tensile test, and fracture toughness can be derived from the area under these curves. Normalized forms of σ–δ expressions are available and appear general enough to describe broad classes of materials. Extensions to include specific mechanisms not accounted for in these models seem feasible.

In ECC material, an enlarged frontal process is responsible for a significant amount of energy

absorption, associated with fiber debonding over a large volume of material, in addition to the wake process available to all FRCs. The order of magnitude of fracture toughness is 0.01 kJ/m^2, 0.1 kJ/m^2, several kJ/m^2, and several tens of kJ/m^2 for cement, concrete, FRC and ECC, respectively. The toughness of the ECC material is competitive with some metallic materials such as aluminum alloys. Under suitable conditions, notch insensitivity can be achieved in ECC and utilized in structural applications.

ACKNOWLEDGEMENTS

Support of the Advanced Civil Engineering Materials Research Laboratory (ACE-MRL) by the National Science Foundation, the National Research Council, Conoco Inc., Shimizu Corporation and the U.S. Gypsum Corporation are gratefully acknowledged.

REFERENCES

1. Bache, H. H., Fracture mechanics in integrated design of new, ultra-strong materials and structures. In *Fracture Mechanics of Concrete Structures, From Theory to Applications*, ed. L. Elfgren. Chapman and Hall, 1989, pp. 383–98.
2. Li, V. C. & Hashida, T., Engineering ductile fracture in brittle matrix composites. *Journal of Materials Science Letters*, **12** (1993) 898–901.
3. Horii, H. & Nanakorn, P., Fracture mechanics based design of SFRC tunnel lining. To appear in *Proc. of JCI International Workshop on Size Effect in Concrete Structures*, ed. H. Mihashi, Sendai, Japan, October 31–November 2, 1993.
4. Naaman, A. E., Reinhardt, H. W. & Fritz, C., Reinforced concrete beams with a SIFCON matrix. *ACI Structural Journal*, **89**(1) (1992) 79–88.
5. Brandt, A. M., Influence of the fibre orientation on the energy absorption at fracture of SFRC specimens. In *Brittle Matrix Composites I*, eds. A. M. Brandt & I. H. Marshall. Elsevier Applied Science Publishers, London, 1986, pp. 403–20.
6. Morton, J., The work of fracture of random fiber reinforced cement. *Materiaux et Constructions*, **12**(71) (1979) 393–6.
7. Shao, Y., Li, Z. & Shah, S. P., Matrix cracking and interface debonding in fiber-reinforced cement–matrix composites. *Journal of Advanced Cement Based Materials*, **1** (1993) 55–66.
8. Leung, C. K. Y. & Li, V. C., Strength based and fracture based approaches in the analysis of fiber debonding. *Journal of Materials Science Letters*, **9** (1990) 1140–2.
9. Aveston, J., Cooper, G. A. & Kelly, A., Single and multiple fracture. In *Properties of Fiber Composites*. IPC Science and Technology Press Ltd, Guildford, UK, 1971, pp. 15–24.
10. Li, V. C., Advances in strain-hardening cement based composites. In *Proc. of Engineering Foundation Conference on Advances in Cement and Concrete*, eds. M. Grutzeck & S. Sarkar. ASCE, New York, 1994.
11. Li, V. C., Post-crack scaling relations for fiber reinforced cementitious composites. *ASCE Journal of Materials in Civil Engineering*, **4**(1) (1992) 41–57.
12. Visalvanich, K. & Naaman, A. E., Fracture modeling of fiber reinforced cementitious composites. Program Report for NSF Grant ENG 77-23534, Department of Materials Engineering, University of Illinois at Chicago Circle, 1982.
13. Wecharatana, M. & Shah, S. P., A model for predicting fracture resistance of fiber reinforced concrete. *Cement and Concrete Research*, **13** (1983) 819–29.
14. Wang, Y., Li, V. C. & Backer, S., Modeling of fiber pull-out from a cement matrix. *International Journal of Cement Composites and Lightweight Concrete*, **10**(3) (1988) 143–9.
15. Leung, C. K. Y. & Li, V. C., Effects of fiber inclination on crack bridging stresses in fiber reinforced brittle matrix composites. *Journal of the Mechanics and Physics of Solids*, **40** (1992) 1333–62.
16. Li, V. C., Wang, Y. & Backer, S., Effect of inclining angle, bundling, and surface treatment on synthetic fiber pull-out from a cement matrix. *Composites*, **21**(2) (1990) 132–40.
17. Li, V. C., Stang, H. & Krenchel, H., Micromechanics of crack bridging in fiber reinforced concrete. *Journal of Materials and Structures*, **26** (1993) 486–94.
18. Maalej, M., Hashida, T. & Li, V. C., Effect of fiber volume fraction on the off-crack-plane fracture energy in strain-hardening engineered cementitious composites. Accepted for publication in the *Jouranl of the American Ceramics Society*, 1994.
19. Mai, Y. W., Failure characterization of fiber reinforced cement composites with R-curve characteristics. In *Toughening Mechanisms in Quasi-Brittle Materials*, ed. S. P. Shah. Kluwer Academic Publishers, Dordrecht, The Netherlands, 1991, pp. 489–527.
20. Li, V. C., Maalej, M. & Lim, Y. M., Fracture and flexural behavior in strain-hardening cementitious composites. In *Proc. of the International Union of Theor. and Appl. Mech. — Symp. on Fracture of Brittle Disorder Materials: Concrete, Rock and Ceramics*, Brisbane, Australia, 20–24 September, 1993.
21. Li, V. C., Chan, C. M. & Leung, C. K. Y., Experimental determination of the tension-softening curve in cementitious composites. *Cement and Concrete Research*, **17**(3) (1987) 441–52.
22. Maalej, M. & Li, V. C., Introduction of strain hardening engineered cementitious composites in the design of reinforced concrete flexural members for improved durability. *ACI Structural Journal*, **92** (2) (1995) 167–176.
23. Wang, Y., Li, V. C. & Backer, S., Tensile properties of synthetic fiber reinforced mortar. *Cement and Concrete Composites*, **12**(1) (1990) 29–40.